A Least-Squares Fitting Technique for Spectral Analysis of Direct and Frequency-Modulation Lineshapes.

Avetisov, Slava

1995

A Least-Squares Fitting Technique for Spectral Analysis of Direct and Frequency-Modulation Lineshapes

Viacheslav G. Avetisov

LRAP-186

Lund Reports on Atomic Physics
1995

A Least-Squares Fitting Technique for Spectral Analysis of Direct and Frequency-Modulation Lineshapes

Viacheslav G. Avetisov

Division of Atomic Physics, Lund Institute of Technology
P.O. Box 118, S-221 00 Lund, Sweden

Abstract

A nonlinear least-squares fitting procedure has been developed to model direct absorption and two-tone frequency-modulation lineshapes using the Voigt, Galatry and Rautian-Sobelman profiles. Details for the lineshape calculations are presented and the iterative least-squares fitting procedure based on the Levenberg-Marquardt method is described.

1. Introduction

A nonlinear least-squares fitting technique is generally employed to determine spectroscopic parameters from high-resolution spectra. The basic approach in all cases is usually the same: a model function with a particular choice of parameters is chosen that is supposed to give the best agreement with data. These parameters are then adjusted using an iterative procedure to minimise the sum of the squares of the differences between observed spectrum and calculated spectrum. This yields the best-fit parameters. For a given experimental spectrum the procedure fits positions, intensities, widths and and/or other parameters of the spectral lines.

In a variety of spectroscopic applications there is a need for quantitative measurements of gas parameters such as concentration, temperature, total pressure, and mixing ratios of molecular and atomic species. In this case, the least-squares fitting technique assumes knowledge of the spectral line parameters, such as line strengths and pressure broadening coefficients to derive the gas parameters.

Two-tone frequency modulation spectroscopy (TTFMS) is a promising technique for gas analysis in industrial and environmental applications. The ability to extract spectral information from TTFMS lineshapes in combination with high sensitivity of the technique

is especially important in the case of measurements in a highly varying environment (e.g. combustion), where variations of the linewidth are significant.

Analytical expressions required for calculations of the spectral profiles and their derivatives are given in Section 2. The analysis is based on the literature and is applicable for both absorption and emission lineshapes. In Section 3 spectral calculations of TTFMS lineshapes are described. Section 4 provides a survey of the very powerful Levenberg-Marquardt method, which today is often used in nonlinear least-squares fitting routines. Section 5 describes the program for spectral calculations and modelling of lineshapes recorded using direct detection and TTFMS.

2. Spectral line profiles

It is convenient to introduce a lineshape function $K(x,y,z)$, which is normalized to the area $\sqrt{\pi}$ and standardized according to Herbert [1]. The dimensionless variables x, y, z are defined in terms of the (possibly shifted) line center ν_0, the Doppler halfwidth σ at $1/e$ intensity, the pressure broadened Lorentzian halfwidth at half maximum (HWHM) Γ (effective state-perturbing collision rate), and the pressure narrowing ξ (effective velocity-changing collision rate):

$x \equiv (\nu - \nu_0)/\sigma$ = standardised frequency deviation from the line centre ν_0,
$y \equiv \Gamma/\sigma$ = standardised broadening parameter,
$z \equiv \xi/\sigma$ = standardised narrowing parameter,
where

$$\sigma \equiv \nu_0 \sqrt{\frac{2kT}{mc^2}}, \tag{2.1}$$

k is the Boltzmann constant, c is the speed of light, T is temperature, and m is the molecular mass.

The dimensionless spectral lineshape $\alpha(\nu - \nu_0)$ can be expressed in terms of a standardised line profile as

$$\alpha(\nu - \nu_0) \equiv S \frac{K(x,y,z)}{\sigma\sqrt{\pi}}, \tag{2.2}$$

where S is the integrated line intensity defined, in the case of absorption, as $S \equiv S_0 P L$, S_0 is the line strength, P is the partial pressure of the absorbing gas, and L is the absorption path length.

In high-resolution spectroscopy, lineshapes are often modelled using a Voigt profile. This profile is a convolution of a Gaussian profile due to Doppler broadening and a

Lorentzian profile due to pressure broadening. The convolution integral defining the Voigt profile can not be evaluated in closed form and therefore has to be computed numerically.

From the convolution integral the Voigt function $V(x,y)$ is given by

$$V(x,y) \equiv \frac{y}{\pi} \int_{-\infty}^{+\infty} \frac{\exp(-t^2)}{(x-t)^2 + y^2} \mathrm{d}t. \tag{2.3}$$

Combining x and y into the complex variable $q \equiv x + iy$, the Voigt function can be represented as the real part $V(x,y) = \mathrm{Re}[w(q)]$ of the complex probability (error) function [2], which for y>0 has the following integral representation

$$w(q) = \frac{i}{\pi} \int_{-\infty}^{+\infty} \frac{\exp(-t^2)}{q-t} \mathrm{d}t, \qquad (y > 0). \tag{2.4}$$

The imaginary part of the complex probability function $L(x,y) = \mathrm{Im}[w(q)]$

$$L(x,y) \equiv \frac{1}{\pi} \int_{-\infty}^{+\infty} \frac{(x-t)\exp(-t^2)}{(x-t)^2 + y^2} \mathrm{d}t \tag{2.5}$$

is related to dispersion and is used also for efficient calculation of the derivatives of the Voigt function.

A fast and accurate (less than 10^{-4} relative error) computer routine for calculation of the real and imaginary parts of the complex probability function $w(q)$ is given by Humlicek [3]. The method is based on rational approximations. It should be mentioned that among different available methods the Humlicek's algorithm is very suitable for molecular spectroscopy, since it provides simultaneously the real and imaginary parts of $w(q)$ [4].

A nonlinear least-squares fitting procedure requires the partial derivatives of the model function with respect to the adjustable parameters as will be shown in Section 4. Using the following differential equation for $w(q)$ [3]

$$w'(q) = \frac{2i}{\sqrt{\pi}} - 2q\,w(q) \tag{2.6}$$

the partial derivatives of the Voigt function with respect to x and y can be obtained as

$$\begin{aligned} \frac{\partial V(x,y)}{\partial x} &= -2\,\mathrm{Re}[q\,w(q)], \\ \frac{\partial V(x,y)}{\partial y} &= 2\,\mathrm{Im}[q\,w(q)] - \frac{2}{\sqrt{\pi}}. \end{aligned} \tag{2.7}$$

For a signal-to-noise ratio (SNR) smaller than 100, the Voigt profile generally provides a good approximation to experimental spectral lineshapes. For a better SNR, systematic deviations originating from collisional (Dicke) narrowing might be observable between experimental lineshapes and the Voigt profile. The manifestation of this effect is most apparent when Doppler broadening and collisional broadening are comparable. Two different models of the molecular (or atomic) collisions successfully describe experimental lineshapes. The "hard" collision model assumes that a single collision entirely changes the velocity of the absorbing (or emitting) molecule, while the "soft" collision model assumes that many collisions are required to change the velocity significantly. The former model yields the Rautian-Sobelman profile [5], and the latter one- the Galatry profile [6]. Although the analytical expressions are different the resulting line profiles are very similar and for experimental accuracy currently achievable either can be used in the modelling.

The standardised Rautian-Sobelman function $R(x,y,z)$ can be represented as the real part $R(x,y,z)=\mathrm{Re}[P(x,y+z)]$ of the complex function [5]

$$P(\tilde{q})\equiv\frac{w(\tilde{q})}{1-\sqrt{\pi}\,z\,w(\tilde{q})}, \tag{2.8}$$

where $\tilde{q}=x+i(y+z)$. Since the complex probability function appears in Eq. (2.8) with just a modified argument, the Humlicek's routine can be used for efficient numerical calculation of the Rautian-Sobelman function.

The partial derivatives of the Rautian-Sobelman functions are obtained as follows

$$\begin{aligned}
\frac{\partial R(x,y,z)}{\partial x}&=\mathrm{Re}\left[\frac{P^2}{w^2}w'\right],\\
\frac{\partial R(x,y,z)}{\partial y}&=-\mathrm{Im}\left[\frac{P^2}{w^2}w'\right],\\
\frac{\partial R(x,y,z)}{\partial z}&=-\mathrm{Im}\left[\frac{P^2}{w^4}w'\right]+\sqrt{\pi}\,\mathrm{Re}\left[\frac{P^2}{w^2}\right],
\end{aligned} \tag{2.9}$$

where $w'(\tilde{q})$ is given by Eq. (2.6). Therefore, the calculation of the Rautian-Sobelman function and its derivatives appears quite efficient for arbitrary x, y, and z.

The Fourier transform of the dipole correlation function for the absorbing molecule that executes Brownian motion yields the following expression for the Galatry function [1,5]

$$G(x,y,z) \equiv \frac{1}{\sqrt{\pi}} \mathrm{Re}\left(\int_0^\infty d\tau \exp\left\{ -ix\tau - y\tau + \frac{1}{2z^2}[\,1 - z\tau - \exp(-z\tau)\,] \right\} \right). \tag{2.10}$$

Using the relation of the Galatry function to the incomplete gamma function, Herbert [1] presented several approximate expressions that, depending on the values of y and z, can be implemented to calculate the Galatry function. For each expression the region of x, y, and z values as well as the number of terms required for 10^{-4} relative error were determined by Varghese and Hanson [7].

The first expression is an asymptotic expansion around the Voigt function, and it can be used for small x, y, and z,

$$G(x,y,z) = \mathrm{Re}\left[w(q) + \sum_{n=3}^{n_1} \frac{c_n}{i^n} \frac{\mathrm{d}^n}{\mathrm{d}q^n} w(q) \right], \qquad n_1 \le 8, \qquad (x \le 2, \quad y \le 0.5, \quad z \le 0.04) \tag{2.11}$$

where

$$c_3 = \frac{z}{2\cdot 3!}, \quad c_4 = -\frac{z^2}{2\cdot 4!}, \quad c_5 = \frac{z^3}{2\cdot 5!}, \quad c_6 = -\frac{z^4}{2\cdot 6!} + \tfrac{1}{2} c_3^2,$$
$$c_7 = \frac{z^5}{2\cdot 7!} + c_3 \cdot c_4, \quad c_8 = -\frac{z^6}{2\cdot 8!} + c_3 \cdot c_5 + \tfrac{1}{2} c_4^2. \tag{2.12}$$

The derivatives of $w(q)$ may be obtained by the following recursion relation for $n \ge 2$

$$\frac{\mathrm{d}^n}{\mathrm{d}q^n} w(q) = -2\left[q \frac{\mathrm{d}^{n-1}}{\mathrm{d}q^{n-1}} w(q) + (n-1) \frac{\mathrm{d}^{n-2}}{\mathrm{d}q^{n-2}} w(q) \right], \tag{2.13}$$

and by Eq. (2.6) for n=1.

The second expression is based on a series expansion of the incomplete gamma function, which can be used for relatively large values of z,

$$G(x,y,z) = \frac{2z}{\sqrt{\pi}} \mathrm{Re}\left\{ \sum_{n=0}^{n_2} \frac{1}{[1+2z(y-ix)][1+2z(y-ix+z)]\cdots[1+2z(y-ix+nz)]} \right\},$$
$$n_2 = 4 + z^{-1.05}[1 + 3\exp(-1.1y)], \qquad (y \le 4z^{0.87}, \quad z \ge 0.1). \tag{2.14}$$

The third expression is based on an approximation of the incomplete gamma function by using a continued fraction, and it can be used for relatively large values of y.

$$G(x,y,z)=\frac{1}{\sqrt{\pi}}\mathrm{Re}\left[\cfrac{1}{y-ix+\cfrac{1\cdot 1/2}{z+y-ix+\cfrac{2\cdot 1/2}{2z+y-ix+\cdots}}}\right],$$

$$n_3 = 2+37\exp(-0.6y), \qquad (2.15)$$

$(y>1,\quad 0.4<z<0.1)$ and $(y>4z^{0.87},\quad z>0.1)$.

The partial derivatives of the Galatry function can be obtained numerically by calculating divided differences.

In modelling spectral lineshapes the following parameters are adjustable: ν_0, S, y, and z. It is important to provide the fitting procedure with good initial values of these parameters. The Doppler halfwidth is calculated from the temperature and absolute wavelength of the transition. The initial value of the line center ν_0 can be easily obtained from the position of the lineshape maximum. The parameter z is generally not very decisive in forming the lineshape and can be set to zero. To provide the initial value of the broadening parameter y the lineshape is assumed to be the Voigt. Various empirical expressions exist for the width of the Voigt profile [8]. A very simple and accurate approximation (better than 0.01 relative error over the whole range of y) was given by Whiting [9]:

$$x_{1/2} \cong y/2+\sqrt{y^2/4+\ln 2}, \qquad (2.16)$$

where $x_{1/2}$ is the standardised Voigt (HWHM). Using this expression the initial value of the broadening parameter can be estimated from the measured HWHM as

$$y \cong x_{1/2}-\frac{\ln 2}{x_{1/2}}. \qquad (2.17)$$

In order to determine the initial value of the integrated line intensity S, a Voigt lineshape can be fitted to the experimental lineshape by using the obtained initial values of ν_0 and y, which are fixed. In the subsequent nonlinear least-squares fitting any of the profiles can be used. It might be useful to perform the first iteration with a Voigt profile, which provides good starting values for the next iteration with a collisionally narrowed profile.

3. Two-tone frequency-modulation lineshape

The characteristic feature of TTFMS is that the laser frequency is modulated by two closely spaced radio frequencies $\nu_1 \equiv \nu_m + \frac{1}{2}\Omega$ and $\nu_2 \equiv \nu_m - \frac{1}{2}\Omega$, while the detection is performed at the beat tone corresponding to the intermediate frequency $\Omega = \nu_1 - \nu_2$. In general, the modulation frequencies are chosen to be comparable or larger than the absorption halfwidth to obtain optimum sensitivity (500-1500 MHz typically), and the intermediate frequency Ω is chosen to be small in comparison with the modulation frequencies but large enough to avoid low-frequency ($1/f$) noise (5-20 MHz typically). This technique preserves high-frequency separation between the sidebands and the carrier, while the heterodyne detection is performed using conventional low-frequency circuits.

For an accurate modelling of high-resolution data obtained by TTFMS, appropriate expressions for calculation of the heterodyne detected signal are essential. The general theory of TTFMS, which is an extension of the previous work by Cooper and Warren [10], has been presented and discussed in details by Avetisov and Kauranen [11].

The TTFMS lineshape associated with the absorption is given by

$$I_\Omega^\alpha = 2I_0 \sum_{n,m} \mathrm{Re}\left(R_{n,m}\right) \exp\left[-\tfrac{1}{2}\left(\alpha_{n,m} + \alpha_{n+1,m-1}\right)\right], \qquad \alpha_{n,m} \equiv \alpha(\nu + n\nu_1 + m\nu_2), \tag{3.1}$$

where I_0 is the laser intensity, and $R_{n,m}$ is a complex function of modulation parameters expressed in terms of Bessel functions as

$$R_{n,m} = r_n r_m r_{n+1}^* r_{m-1}^* + J_{n+1}(\beta) J_{m-1}(\beta) A_{n,m} + J_n(\beta) J_m(\beta) A_{n+1,m-1}^*, \tag{3.2}$$

where

$$r_n(\beta, M, \psi) \equiv J_n(\beta) + \frac{M}{2i}\left[J_{n-1}(\beta)\exp(i\psi) - J_{n+1}(\beta)\exp(-i\psi)\right], \tag{3.3}$$

β is the frequency modulation (FM) index, M is the amplitude modulation (AM) index, ψ is the phase difference between AM and FM, and $A_{n,m}$ is a corrective term due to nonlinear distortion in the frequency modulation response of the diode laser. It has been shown [11] that for an accurate modelling of TTFMS lineshapes it is sufficient to account only for the second-order harmonic distortion. The corrective term for this case is

$$A_{n,m} \equiv J_m(\beta)\delta_n + J_n(\beta)\delta_m, \tag{3.4}$$

where

$$\delta_n(\beta,\zeta,\vartheta) \equiv J_{n-2}(\beta)\, J_1(\zeta) \exp(i\vartheta) + J_{n+2}(\beta)\, J_{-1}(\zeta) \exp(-i\vartheta), \tag{3.5}$$

ζ and ϑ are the second-harmonic amplitude and phase shift, respectively.

For the expression (3.1) to be accurate with 10^{-3} relative error the following requirements were obtained

$$\alpha(\nu_0)\frac{\Omega}{\Delta} < 4\times10^{-3}, \quad \frac{\Omega}{\Delta} < 0.2, \tag{3.6}$$

which are generally fulfilled in practice.

The expressions presented above can be simplified by applying the approximation $\nu_1 \approx \nu_2 \approx \nu_m$. The TTFMS lineshape is then represented as

$$I_\Omega^\alpha = 2I_0 \sum_{n,m} \mathrm{Re}\left(R_{n,m}\right) \exp\left\{-\alpha\left[\nu + (n+m)\,\nu_m\right]\right\}, \tag{3.7}$$

where

$$R_{n,m} = r_n\, r_m\, r_{n+1}^*\, r_{m-1}^* + \left[\, J_{n+1}(\beta) J_{m-1}(\beta) + J_{n-1}(\beta) J_{m+1}(\beta)\,\right] A_{n,m}. \tag{3.8}$$

The expression (3.7) is accurate with 10^{-3} relative error if

$$\frac{\Omega}{\Delta} < \frac{0.02}{1+\left(\Delta/\nu_m\right)^2}. \tag{3.9}$$

The maximum values of n and m required for the calculation of the lineshape by Eqs. (3.1) and (3.7) with a 10^{-3} relative error can be determined for moderate FM indices (β <1.5) using the following empirical relations:

$$|n| \le 4, \quad |m| \le 4, \quad |n| + |m| \le 2 + 2.3\beta. \tag{3.10}$$

For simplicity, the dc offset $c\varepsilon_0 E_0^2 M^2$ due to the AM is eliminated in the calculated lineshapes by subtraction. The absorption of a sideband at frequency $\nu_c + n\,\nu_1 + m\,\nu_2$ is computed according to

$$\alpha_{n,m} \equiv S\,\frac{K(x + n\bar{\nu}_1 + m\bar{\nu}_2, y, z)}{\sigma\sqrt{\pi}}, \tag{3.11}$$

where $\bar{\nu}_1 \equiv \nu_1/\sigma$ and $\bar{\nu}_2 \equiv \nu_2/\sigma$. When using Eq. (3.7) one approximates $n\bar{\nu}_1 + m\bar{\nu}_2 \cong (n+m)\bar{\nu}_m$, where $\bar{\nu}_m \equiv \nu_m/\sigma$. Thus, five modulation parameters β, M, ψ, $\bar{\nu}_1$ and $\bar{\nu}_2$ and five spectroscopic parameters S, y, z, ν_0 and σ determine a TTFMS lineshape. Normally, the values of σ, $\bar{\nu}_1$, and $\bar{\nu}_2$ (or $\bar{\nu}_m$) are well known, and it was

shown [11] that setting $\psi=\pi/2$ is generally a good approximation. The phase shift of the harmonic distortion is generally $\vartheta=\pi$ in diode lasers [12] and can be fixed, while the amplitude ζ might be either set manually or adjusted in the final iteration (typically ζ =0.01-0.03). Thus, the principal parameters to be adjusted are S, y, z, ν_0, β, and M.

The partial derivatives with respect to S, y, z, ν_0 are easily obtained by multiplying each term in Eq. (3.1) or (3.7) to the corresponding derivative of the lineshape function $\frac{\partial K(x+n\bar{\nu}_1+m\bar{\nu}_2,y,z)}{\partial a_i}$,

where a_i is either the S, y, z, and ν_0 parameters. The Bessel functions are computed using the recurrence formula

$$J_{n+1}(\beta)=\frac{2n}{\beta}J_n(\beta)-J_{n-1}(\beta), \tag{3.12}$$

and the derivatives of the Bessel functions required in the least-squares fitting procedure for adjusting the FM index β are calculated as

$$\frac{dJ_n(\beta)}{d\beta}=\tfrac{1}{2}[J_{n-1}(\beta)-J_{n+1}(\beta)]. \tag{3.13}$$

The partial derivative of $R_{n,m}$ with respect to β and M are computed according to

$$\frac{\partial R_{n,m}}{\partial a_j}=\left(\frac{\partial r_n}{\partial a_j}r_m+\frac{\partial r_m}{\partial a_j}r_n\right)r^*_{n+1}r^*_{m-1}+\left(\frac{\partial r^*_{n+1}}{\partial a_j}r^*_{m-1}+\frac{\partial r^*_{m-1}}{\partial a_j}r^*_{n+1}\right)r_n r_m, \tag{3.14}$$

where a_j is either β or M.

The initial value for the FM index can be estimated experimentally e.g. from the relative ratio of the sidebands and the carrier component obtained from a spectrum of direct transmission of a high-finesse Fabry-Perot etalon. The amplitude of the k-ht. sideband component (k=0 for the carrier component) is given by

$$I_k \propto \sum_n |r_n|^2 |r_{k-n}|^2. \tag{3.15}$$

Table 1 lists the peak amplitude ratio of four successive sidebands to the carrier component as a function of the FM index β, which might be of help when estimating β.

Table 1. The sideband-to-carrier ratio in the Fabry-Perot transmission spectrum as a function of the FM index β calculated using Eq. (3.15) with M=0 and ζ=0.

β	I_1/I_0	I_2/I_0	I_3/I_0	I_4/I_0
0.1	0.005	0	0	0
0.2	0.020	0.0002	0	0
0.3	0.046	0.0008	0	0
0.4	0.083	0.0026	0	0
0.5	0.132	0.0065	0.0002	0
0.6	0.194	0.014	0.0005	0
0.7	0.270	0.027	0.0013	0
0.8	0.357	0.049	0.003	0.0001
0.9	0.454	0.081	0.007	0.0003
1.0	0.555	0.127	0.013	0.0008
1.1	0.648	0.187	0.024	0.002
1.2	0.722	0.260	0.042	0.004
1.3	0.763	0.338	0.066	0.007
1.4	0.767	0.413	0.096	0.012
1.5	0.735	0.475	0.133	0.020
1.6	0.679	0.519	0.172	0.030
1.7	0.613	0.543	0.213	0.043
1.8	0.552	0.549	0.254	0.060
1.9	0.503	0.543	0.295	0.080
2.0	0.471	0.527	0.334	0.105

The initial value of the AM index can be set to zero [11]. An estimation of the broadening parameter is not so straightforward. If the FM index is estimated, an arbitrary guess of y can be used in the first iteration with the Voigt profile. More accurately, the Voigt HWHM can be estimated from a TTFMS lineshape using the empirical expression

$$x_{1/2} = (\Delta_x - \bar{\nu}_m - \tfrac{1}{2}\beta)\cdot 0.55 - 0.2, \tag{3.16}$$

where Δ_x is the standardised distance between the two minima of the TTFMS lineshape. The expression provides a better than 10% estimate of the HWHM for $\bar{\nu}_m \le 2$ and $\beta \le 1.2$. Then the broadening parameter can be calculated by Eq. (2.17). The initial value of the line center ν_0 is provided by the position of the lineshape maximum, and the parameter z can be initially set to zero.

4. Nonlinear least-squares

A least-squares fitting procedure involves using a model spectrum $M = M(x;\mathbf{a})$, which is a function of the standardised frequency x and a vector of parameters $\mathbf{a} = (a_1, a_2, \ldots a_J)$, where J is the number of parameters. These parameters are adjusted until the best fit between the model M and observed data D is achieved. To determine the best-fit parameters one have to minimise a sum-of-squares deviation parameter ρ (variance) defined as

$$\rho(\mathbf{a}) = \sum_{i}^{N} \left[D_i - M(x_i, \mathbf{a}) \right]^2, \tag{4.1}$$

where N is the number of data points.
Expanding ρ in a Taylor series up to a quadratic term yields

$$\begin{aligned} \rho(\mathbf{a}+\delta\mathbf{a}) &= \rho(\mathbf{a}) + \sum_{k}^{J} \frac{\partial \rho}{\partial a_k} \delta a_k + \frac{1}{2} \sum_{k,l}^{J} \frac{\partial^2 \rho}{\partial a_k \partial a_l} \delta a_k \delta a_l \\ &= \rho(\mathbf{a}) - \mathbf{b} \cdot \delta\mathbf{a} + \delta\mathbf{a} \cdot \mathbf{A} \cdot \delta\mathbf{a}, \end{aligned} \tag{4.2}$$

where

$$\mathbf{b} \equiv -\nabla\rho(\mathbf{a}), \quad A_{k,l} \equiv \frac{1}{2} \frac{\partial^2 \rho}{\partial a_k \partial a_l}\bigg|_{\mathbf{a}}. \tag{4.3}$$

In the approximation (4.2) the gradient of $\rho(\mathbf{a}+\delta\mathbf{a})$ is calculated as

$$\nabla\rho(\mathbf{a}+\delta\mathbf{a}) = \mathbf{A} \cdot \delta\mathbf{a} - \mathbf{b}. \tag{4.4}$$

If the model M is linear in $\mathbf{a}$ and the parameters are independent, the minimum of the approximate function $\rho(\mathbf{a})$ given by Eq. (4.2) is at $\mathbf{a}+\delta\mathbf{a}$ [13], where

$$\delta\mathbf{a} = \mathbf{A}^{-1} \cdot \mathbf{b}. \tag{4.5}$$

In a nonlinear case, the system of linear equations (4.5) gives a new parameter set $\mathbf{a}+\delta\mathbf{a}$, which is somewhat closer to the minimum than the initial parameter set $\mathbf{a}$. The function ρ is then expanded around the new values by Eq. (4.2). The procedure is iteratively repeated until ρ stops decreasing.

By differentiating Eq. (4.1) $\mathbf{A}$ and $\mathbf{b}$ can be expressed explicitly in terms of the model function M as

$$b_k = -\frac{\partial \rho}{\partial a_k} = 2\sum_{i=1}^{N}\left[D_i - M(x_i,\mathbf{a})\right]\frac{\partial M(x_i,\mathbf{a})}{\partial a_k} \qquad (k = 1,2,\ldots,J) \tag{4.6}$$

and

$$A_{k,l} = \frac{1}{2}\frac{\partial^2 \rho}{\partial a_k \partial a_l} = \sum_{i=1}^{N}\left\{\frac{\partial M(x_i,\mathbf{a})}{\partial a_k}\frac{\partial M(x_i,\mathbf{a})}{\partial a_l} - \left[D_i - M(x_i,\mathbf{a})\right]\frac{\partial^2 M(x_i,\mathbf{a})}{\partial a_l \partial a_k}\right\}. \tag{4.7}$$

Near the minimum of the function $\rho(\mathbf{a})$, the term $\left[D_i - M(x_i,\mathbf{a})\right]$ in Eq. (4.7) tends to zero and is just the random measurement error for each data point. For this reasons the second derivatives in Eq. (4.7) are generally ignored, which greatly simplifies calculations. The matrix elements of **A** are then given by

$$A_{k,l} = \sum_{i=1}^{M}\frac{\partial M(x_i,\mathbf{a})}{\partial a_k}\frac{\partial M(x_i,\mathbf{a})}{\partial a_l}. \tag{4.8}$$

Thus, the Taylor expansion method is applicable near the minimum of the function $\rho(\mathbf{a})$. For each iteration step, the system of linear equations (4.5) with matrices **b** and **A** given by Eqs. (4.6) and (4.8), respectively, is solved.

Far from the minimum the Taylor expansion is a poor approximation and may destabilise the fitting procedure yielding a larger value of $\rho(\mathbf{a})$ with each iteration. In this case a gradient search method, which involves using only the diagonal elements of the matrix **A**, is more appropriate, since it will always find a smaller value of ρ. If the model M is linear with **a**, the minimum of $\rho(\mathbf{a})$ in the direction of the gradient $\nabla\rho(\mathbf{a})$ is given by [13]

$$\delta a_k = \frac{b_k}{A_{kk}} \qquad k = 1,2,\ldots,J. \tag{4.9}$$

In a nonlinear case, the gradient $\nabla\rho(\mathbf{a})$ yields the direction of the greatest change of ρ, which is however not always the direction to the minimum. Moreover, by Eq. (4.9) the gradient might yield too big change of the parameter vector **a**. To stabilise the fitting process it is, thus, useful to reduce the obtained step $\delta\mathbf{a}$ by some factor.

The Levenberg-Marquardt method [14] involves using the gradient search (4.9) far from the minimum and the Taylor expansion (4.5) near the minimum of $\rho(\mathbf{a})$. The transition between these methods varies smoothly as the minimum is approached. Accordingly, the matrix **A** in Eq.(4.5) is replaced by **A'**

$$\mathbf{A}' \cdot \delta\mathbf{a} = \mathbf{b} \tag{4.10}$$

which is given by

$$A'_{kl} = \begin{cases} A_{kl} & k \neq l \\ (1+\lambda)A_{kk} & \end{cases} . \qquad (4.11)$$

For large values of λ, the matrix **A'** is constrained to be diagonal, which means that the method is identical to the gradient search [Eq.(4.9)] except the step size is reduced by the factor $1/(1+\lambda)$. For $\lambda<<1$, **A'=A** and the method is identical to the Taylor expansion.

The fitting process can be started using e.g. $\lambda=0.01$. When the set of linear equations (4.10) is solved and $\rho(\mathbf{a}+\delta\mathbf{a})$ is evaluated, λ is either multiplied or divided by a factor (e.g. 10) depending on whether $\rho(\mathbf{a}+\delta\mathbf{a})$ appears to be larger or smaller than $\rho(\mathbf{a})$.

The method has proven itself as very flexible, fast and reliable, and has become commonly used in nonlinear least-squares procedures.

5. The program structure

The program for spectral analysis is written using Turbo-Pascal for the MS-DOS operating system as a sequence of small, relatively independent modules, which makes it easy to test and modify for solving different tasks. The program can be used for least-squares fitting and simulation of direct detected and TTFMS spectra. Any structural performance of the program, e.g., simulation and modelling of spectra, calculations of calibration curves, data input and output, etc., can be easily accomplished by changing the body of the main program. Since least-squares fitting of high-resolution spectra is a matter of "art" which requires skills, this approach seems to be more flexible than trying to design an executable version of the program with an extended interface that fulfils all requirements. The modular structure of the program makes it possible for the user to build up his own routines for solving a particular task. Therefore, the program is directed to those who has some experience in high-resolution spectroscopy and programming, however, only elementary knowledge of the Pascal language is required for simple implementations.

The general structure of the program is shown in Fig. 1. The program contains four units, and each unit contains procedures for different purposes. All procedures that are required for handling of the program are located in the Main program. Unit1 performs one iteration of the Levenberg-Marquardt method. Unit2 contains the procedures for the calculation of lineshapes and their derivatives with respect to adjustable parameters. Unit3 utilises arithmetic of a complex variable, which is not inherently presented in Pascal. This makes the calculation of lineshapes more simple and fast. Below we will specify the purpose of different parts and procedures in more details.

The important global variables that are used by different parts of the program are

D[1..*ndata*] - array of data to be fitted,

x[1..*ndata*] - array of standardised frequency,

a[1..*na*,1..*nl*] - *na*×*nl* array of parameters, where *na* is the total number of parameters for a lineshape and *nl* is the number of spectral lines included in the model,

l[1..*na*,1..*nl*] - *na*×*nl* array of Boolean variables showing the parameters to be adjusted,

bs[-*m*..*m*] - array of Bessel functions of up to *m*-th order,

M_i - model function calculated at the *i*-th point,

$\partial M_i / \partial \mathbf{a}[1..na, 1..nl]$ - array of derivatives of the model function at the *i*-th point.

ρ - variance.

The Main program contains the following procedures:

READDATA- reads specified binary data file (2 byte integer) into the array ***D*** [1..*ndata*];

READINIT- reads a previously stored text file that contains the initial values of the parameters and supplementary information, which includes:

list of parameters **l**[1..*na*,1..*nl*] to be adjusted;

spectrum type (Direct, TTFMS1, or TTFMS2),

line profile to be used (Voigt, Rautian-Sobelman, or Galatry),

frequency increment of data points,

transition frequency and sample temperature (for the calculation of the theoretical Doppler width),

modulation frequencies ν_1 and ν_2, AM-FM phase difference ψ, harmonic distortion amplitude ζ and phase shift ϑ (for TTFMS only);

WRITEINIT- stores initial values of the parameters and the supplementary information into the text file;

FINDMINMAX- searches for minima and maxima of a data array and least-squares fits parabolas to the data in the regions around the determined positions; determines the width of a direct absorption lineshape, the distance between the two minima and the peak-to-peak value of a TTFMS lineshape;

CALCINIT- calculates initial parameters by expressions (2.17) and (3.16);

CALCSPEC- calculates a spectrum for a current set of parameters;

FITSPEC- a driver for Unit1; performs a least-squares fitting to data with given initial parameters and returns a set of the best-fit parameters;

VIEWSPEC- wiews the observed and calculated spectra and the residual between them;

WRITEOUT- writes the calculated spectrum into a binary (or text) file, and the best fit parameters and additional information into a text file.

The body of the Main program specifies the required implementation. For example, the text written in the BODY-box in Fig. 1 is a simplified form of the implementation for fitting several spectra consecutively using the same initial parameters for each spectrum. The result of each fit is is stored.

Unit1 performs one iteration of the least-squares fit. It contains several procedures [14] for solving linear equations (4.10) and calculating ρ. Upon each call to the unit the best-fit parameters, the corresponding ρ, and the suggested value of λ for the next iteration are returned.

Unit2 contains a set of procedures that are used to calculate the model at a given point x_i :

BESSEL- calculates Bessel functions for a given argument (only for TTFMS);

CPF- calculates the real and imaginary parts of the complex probability function $w(x_i,y)$ by the Humlichek's algorithm;

VOIGT- calculates the Voigt function and its derivatives;

RAUT_SOBEL- calculates the Rautian-Sobelman function and its derivatives;

GALATRY- calculates the Galatry function and its derivatives;

TTFMS1- calculates the TTFMS lineshape by Eq. (3.1) and its derivatives using either of the line profiles;

TTFMS2- calculates the TTFMS lineshape by Eq. (3.7) and its derivatives using either of the line profiles;

FUNCTION- a driver for the calculation of the model; selects the procedures and builds up the total value of the model function by adding the contribution from different spectral lines.

The modular structure of the program allows new procedures to be added to the Main program for handling purposes. Other line profiles, e.g. generilised Galatry and Rautian-Sobelman profiles, and lineshapes, e.g. WMS FMS lineshapes, can also be implemented by adding the corresponding procedures to Unit2. For example, a procedure for calculating WMS lineshapes (2*f* detection) is under development and will soon be available.

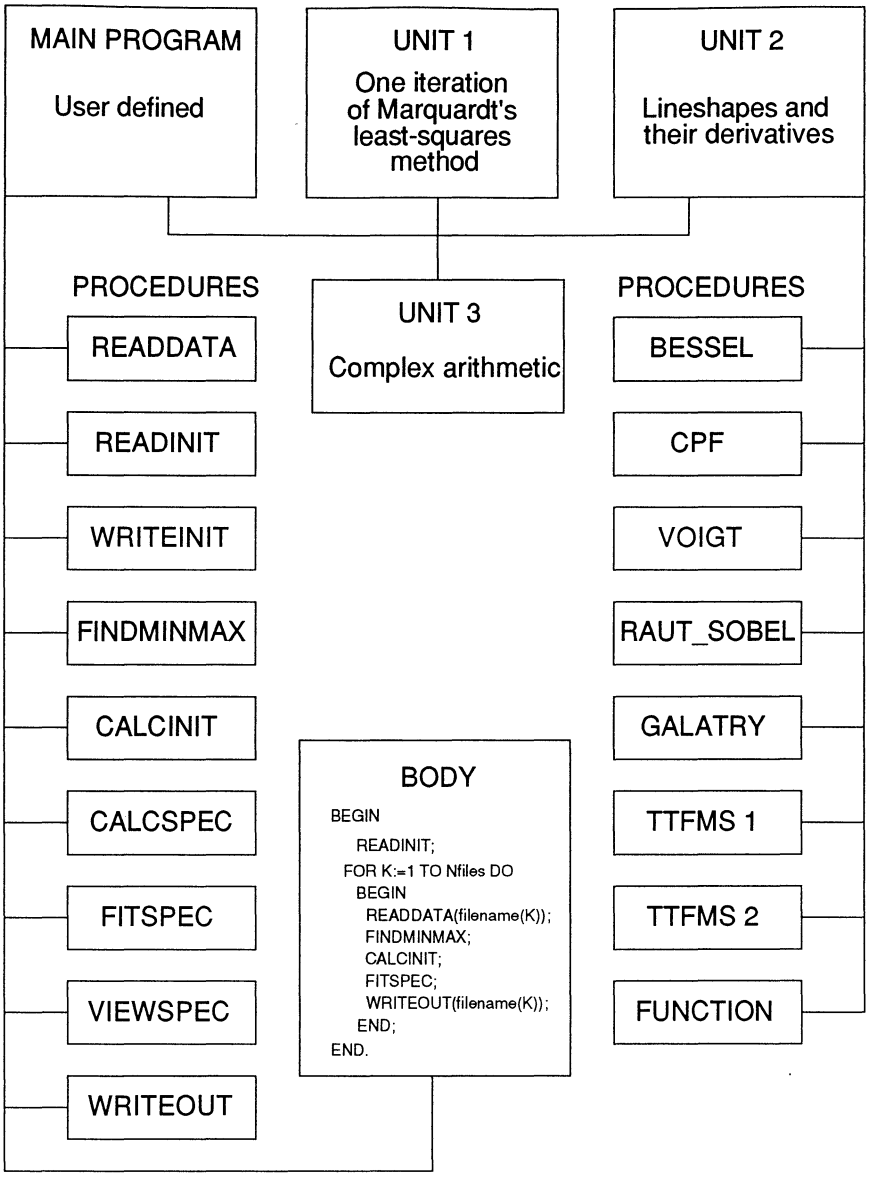

Fig. 1 Block scheme of the least-squares fitting program.

References

1. F. Herbert, "Spectrum line profiles: a generalized Voigt function including collisional narrowing," J. Quant. Spectrosc. Radiat. Transfer **14**, 943-951 (1974).
2. M. Abramowitz and I. A. Stegun, *Handbook of Mathematical Functions*, Dover, New York (1972).
3. J. Humlicek, "Optimized computation of the Voigt and complex probability functions," J. Quant. Spectrosc. Radiat. Transfer **27**, 437-444 (1982).
4. F. Schreier, "The Voigt and complex error function: a comparison of computational methods," J. Quant. Spectrosc. Radiat. Transfer **48**, 743-762 (1992).
5. S. G. Rautian and I. I. Sobelman, "Effect of collisions on the Doppler broadening of spectral lines," Sov. Phys. Usp. **9**, 701-716 (1967).
6. L. Galatry, "Simultaneous effect of Doppler and foreign gas broadening on spectral shapes," Phys. Rev. **122**, 1218-1223 (1961).
7. P. V. Varghese and R. K. Hanson, "Collisional narrowing effects on spectral line shapes measured at high resolution," Appl. Opt. **23**, 2376-2385 (1984).
8. J. J. Olivero and R. L. Longbothum, "Empirical fits to the Voigt line width: a brief review," J. Quant. Spectrosc. Radiat. Transfer **17**, 233-236 (1977).
9. E. E. Whiting, "An empirical approximation to the Voigt profile," J. Quant. Spectrosc. Radiat. Transfer **8**, 1379-1384 (1968).
10. D. E. Cooper and R. E. Warren, "Two-tone optical heterodyne spectroscopy with diode lasers: theory of line shapes and experimental results," J.Opt.Soc.Am. **B4**, 470-480 (1987).
11. V. G. Avetisov and P. Kauranen, "Two-tone frequency modulation spectroscopy for quantitative measurements of gaseous species: theoretical, numerical and experimental investigation of lineshapes," submitted to Appl. Opt. (1995).
12. G. Morthier, F. Libbrecht, K. David, P. Vankwikelberge, and R. G. Baets, "Theoretical investigation of the second-order harmonic distortion in the AM response of 1.55 μm F-P and DFB lasers," IEEE J. Quant. Electron. **27**, 1990-2002 (1991).
13. P. R. Bevington, *Data Reduction and Error Analysis for the Physical Sciences*, McGraw-Hill, New York (1969).
14. W. H. Press, B. P. Flannery, S. A. Teukolsky, and W. T. Vetterling, *Numerical Recipes*, Cambridge University Press, Cambridge (1989).